

# Oxidation of Activated Carbon Fibers: Effect on Pore Size, Surface Chemistry, and Adsorption Properties

Christian L. Mangun,\* Kelly R. Benak, Michael A. Daley, and James Economy

Department of Materials Science and Engineering, 1304 W. Green Street,  
Urbana, Illinois 61801

Received March 1, 1999. Revised Manuscript Received October 8, 1999

Activated carbon fibers (ACFs) were oxidized using both aqueous and nonaqueous treatments. As much as 29 wt % oxygen can be incorporated onto the pore surface in the form of phenolic hydroxyl, quinone, and carboxylic acid groups. The effect of oxidation on the pore size, pore volume, and the pore surface chemistry was thoroughly examined. The average micropore size is typically affected very little by aqueous oxidation while the micropore volume and surface area decreases with such a treatment. In contrast, the micropore size and micropore volume both increase with oxidation in air. Oxidation of the fibers produces surface chemistries in the pore that provide for enhanced adsorption of basic (ammonia) and polar (acetone) molecules at ambient and nonambient temperatures. The adsorption capacity of the oxidized fibers for acetone is modestly better than the untreated ACFs while the adsorption capacity for ammonia can increase up to 30 times compared to untreated ACFs. The pore surface chemical makeup was analyzed using elemental analysis, diffuse reflectance infrared Fourier transform spectroscopy (DRIFTS), and X-ray photoelectron spectroscopy (XPS).

## Introduction

One of the undesirable features of the modern day world is widespread contamination associated with the release of a large number of chemicals into the environment. In recent years there has been a tremendous amount of work done to quantify the harmful effect of these trace contaminants. Society's growing concern has led many governments to establish stricter standards for clean air and water, many of them in the parts per billion range. This necessitates the development of greatly improved methods for controlling the release of toxic contaminants and on designing new materials tailored to selectively remove a wide range of contaminants and permit for recovery and reuse. One technology that is extremely attractive for this purpose is the use of adsorbents such as ACFs. These materials provide a number of advantages over granular carbon including simplified containment, capability for in situ regeneration through electrical resistance heating, and greater rates of adsorption due to improved contact efficiency.

In this research paper, we examine how tailoring the pore surface chemistry through oxidation affects the microstructure of ACFs and enhances adsorption of specific contaminants. Methods for the oxidation of activated carbon have been well-documented in literature. Previous researchers have used air, water vapor, nitric acid, or a mixture of nitric and sulfuric acids to carry out oxidation reactions.<sup>1,2</sup> The effect of oxidation

on surface area and micropore volume of carbon granules was studied by Barton et al. while Boehm developed a titration method to separate the contributions from different acidic groups.<sup>3,4</sup> However, few authors have described the effects of oxidation on adsorption of gaseous contaminants. Earlier work in our laboratory has shown that posttreatment of ACFs in concentrated nitric/sulfuric acid produces a highly oxidized pore structure but studies with saturated gases did not indicate a more effective adsorbent.<sup>5</sup> Tamon and co-workers examined the influence of surface oxides of granular carbon on gas adsorption, and this study will be used to compare the adsorption characteristics of granular versus fibrous activated carbon.<sup>6</sup> To our knowledge, this is the first paper to detail how adsorption of polar and basic contaminants by high surface area ACFs can be enhanced through various oxidation methods.

## Experimental Section

**Preparation of Fiber Samples.** The samples used in this study consisted of activated carbon fibers with various surface areas. Nippon Kynol commercially prepared these fibers by carbonizing and activating a phenolic fiber precursor (Kynol) in steam/carbon dioxide. The preparation of these materials is extensively described in the literature.<sup>7</sup> The fibers used in

\* To whom correspondence should be sent. E-mail: c-mangun@uiuc.edu. Phone: 217-244-2523. Fax: 217-333-2736.

(1) Puri, B. R. Surface Complexes on Carbon. In *Chemistry and Physics of Carbon*; Walker, P. L., Jr., Ed.; A Series of Advances; Marcel Dekker: New York, 1970; Vol. 6, pp 191–275.

(2) Ermolenko, I. N.; Lyubliner, I. P.; Gulko, N. V. Surface Modification of Carbon Fibers. *Chemically Modified Carbon Fibers and Their Applications*; VCH Publishers: New York, 1990; pp 155–199.

(3) Barton, S. S.; Evans, M. J. B.; MacDonald, J. A. F. *Adsorpt. Sci. Technol.* **1993**, *10*, 75.

(4) Boehm, H. P. In *Advances in Catalysis*; Eley, D. D., Pines, H., Weisz, P. B., Eds.; Academic Press: New York, 1966; Vol 16

(5) Economy, J.; Foster, K.; Andreopoulos, A.; Jung, H. *CHEMTECH* **1992**, *22* (10), 597.

(6) Tamon, H.; Okazaki, M. *Carbon* **1996**, *34* (6), 741.

(7) Lin, R. Y.; Economy, J. *J. Appl. Polym. Symp.* **1973**, *21*, 143.

**Table 1. Pore Size, Pore Volume, and Surface Area of Oxidized ACFs and Their Untreated Precursors<sup>a</sup>**

| sample | treatment   | % C  | % H  | % O  | BET SA (m <sup>2</sup> /g) | pore width (Å) | micropore vol (mL/g) |
|--------|---|------|------|------|----------------------------|----------------|----------------------|
| ACF-10 | untreated   | 92.4 | 0.76 | 6.63 | 738                        | 5.4            | 0.319                |
| 10-A1  | concd H <sub>2</sub> SO <sub>4</sub> /HNO <sub>3</sub> mixture for 10 min | 74.0 | 1.55 | 21.5 | 547                        | 5.7            | 0.235                |
| 10-A2  | concd H <sub>2</sub> SO <sub>4</sub> /HNO <sub>3</sub> mixture for 60 min | 70.6 | 0.83 | 26.5 | 531                        | 6.4            | 0.229                |
| ACF-15 | untreated   | 95.2 | 0.24 | 4.33 | 1390                       | 10.2           | 0.600                |
| 15-A1  | concd H <sub>2</sub> SO <sub>4</sub> /HNO <sub>3</sub> for 10 min         | 74.8 | 1.27 | 22.5 | 1263                       | 10.2           | 0.542                |
| 15-A2  | concd H <sub>2</sub> SO <sub>4</sub> /HNO <sub>3</sub> for 60 min         | 68.2 | 1.89 | 28.4 | 1137                       | 10.6           | 0.475                |
| 15-C1  | concd HNO <sub>3</sub> at 25 °C for 60 min                                | 85.7 | 0.63 | 13.0 | 1296                       | 9.8            | 0.552                |
| 15-C2  | boiling HNO <sub>3</sub> for 60 min                                       | 69.4 | 0.96 | 29.0 | 976                        | 10.3           | 0.403                |
| 15-D1  | 30% H <sub>2</sub> O <sub>2</sub> at 25 °C for 60 min                     | 88.6 | 1.41 | 9.67 | 1293                       | 10.5           | 0.554                |
| 15-E1  | concd CH <sub>3</sub> COOH at 25 °C for 60 min                            | 90.4 | 1.84 | 7.79 | 1388                       | 10.3           | 0.593                |
| 15-F1  | air at 400 °C for 30 min  | 84.5 | 0.67 | 14.8 | 1575                       | 10.9           | 0.662                |
| 15-F2  | 10% air/N <sub>2</sub> at 600 °C for 30 min                               | 76.8 | 0.65 | 22.6 | 1785                       | 13.2           | 0.670                |
| ACF-25 | untreated   | 95.6 | 0.15 | 4.02 | 1960                       | 12.5           | 0.785                |
| 25-A1  | concd H <sub>2</sub> SO <sub>4</sub> /HNO <sub>3</sub> for 10 min         | 71.5 | 1.31 | 26.0 | 1620                       | 11.9           | 0.635                |
| 25-A2  | concd H <sub>2</sub> SO <sub>4</sub> /HNO <sub>3</sub> for 60 min         | 69.3 | 1.57 | 27.9 | 1313                       | 11.4           | 0.511                |

<sup>a</sup> The effect of oxidation on the chemical composition is shown from the use of elemental analysis.

this study were designated ACF-10, ACF-15, and ACF-25 having Brunauer, Emmett, and Teller (BET) surface areas of 738, 1390, and 1960 m<sup>2</sup>/g, respectively. These fibers were subsequently oxidized using the treatments described in Table 1.

For the aqueous treatments, typically a 0.3–0.9 g of sample was placed into a 150-mL beaker and reacted with 100 mL of the oxidizing agent under the conditions stated in Table 1. To ensure removal of excess oxidant, samples were washed with distilled water at least 5 times with continuous stirring. Samples were then dried under vacuum at 125 °C for 12 h.

Air-oxidized ACF samples were prepared in a 5-cm diameter quartz tube with ground glass end caps which was placed in a Lindberg tube furnace. All air flow rates were 200 mL/min with other reaction conditions described in Table 1. Immediately following air oxidation the fibers were cooled to room temperature in argon at a flow rate of 2 L/min.

**Nitrogen Adsorption/Surface Area Calculation.** A Coulter Omnisorb 100 (Hiialeah, FL) was used for the volumetric measurement of nitrogen adsorption isotherms at 77 K. The ACFs were degassed for 24 h under vacuum at 150 °C. The nitrogen adsorption experiments were performed in static mode using a mass flow controller that was programmed to supply a fixed dose of nitrogen to the sample container. After equilibration, the pressure was recorded and the process was continued at higher dose pressures until the saturation pressure was reached. The pressure difference between the previous pressure measurement and the next equilibrated pressure along with the dose volume was used to calculate the amount of nitrogen adsorbed by the sample. Surface area values were calculated from the experimental adsorption isotherm over a relative pressure range of 0.01 to 0.20 using the standard Brunauer, Emmett, and Teller (BET) method.

**Micropore Size Analysis.** The Dubinin–Radushkevich equation was applied to the nitrogen experimental isotherm at 77 K.<sup>8</sup> From these data, the micropore width ( $L$ ) and the micropore volume ( $W_0$ ) can be determined. The following equations were used:

$$\log(W) = \log(W_0) + M(\log^2(P_0/P)) \quad (1)$$

where  $W$  is the amount of gas/vapor adsorbed (in mL/g),  $P/P_0$  is the concentration of the adsorbate,  $W_0$  is the micropore volume as calculated from the intercept of a  $\log(W)$  vs  $\log^2(P_0/P)$  plot while  $M$  is the slope of the best fit line and corresponds to

$$M = -2.303(RT/E)^2 \quad (2)$$

where  $R$  is the ideal gas constant,  $T$  is the temperature (in Kelvin), and  $E$  is the energy of adsorption. Assuming a slit-

shaped pore, the micropore half-width may be calculated using the following equation:

$$x = \beta k/E \quad (3)$$

where  $k$  is a constant, and  $x$  is the micropore half width. The similarity coefficient  $\beta$  is a shifting factor that depends only on the adsorbate and is equal to  $E/E_0$ , where  $E_0$  is the adsorption energy of a reference vapor (typically benzene). For nitrogen,  $\beta$  is equal to 0.33 and  $k$  is a structural parameter which is equal to 13 nm kJ/mol for this set of materials.<sup>9</sup> The micropore width,  $L$ , is calculated as twice the micropore half-width,  $x$ .

**Elemental Analysis.** Elemental analysis was performed using a Model 240XA Elemental Analyzer (Control Equipment Corporation). The nitrogen, carbon, hydrogen, and sulfur content were determined directly while the oxygen content was calculated by difference. For brevity, nitrogen and sulfur contents were not reported in Table 1 since the amount of these elements was not significant (<1%).

**XPS.** X-ray photoelectron spectroscopy (XPS) was used to determine the number and type of functional groups present on the surface of the oxidized ACFs. XPS spectra were obtained using a Physical Electronics PHI 5400 XPS spectrophotometer with an achromatic Mg K $\alpha$  X-ray source. The spectrometer was calibrated using Cu and Au lines with known peak separations. The carbon C1s electron binding energy corresponding to graphitic carbon was referenced at 284.6 eV for calibration purposes. Prior to examination, the samples were dried at 150 °C under vacuum to remove adsorbed contaminants. XPS was run in the retarding mode using a survey pass energy of 178.95 eV and a multiplex pass energy of 17.9 eV. Previous researchers have established that decomposition of surface oxides does occur on exposure to X-rays.<sup>10</sup> Thus, spectra were recorded for a fixed time of 20 min to minimize these effects. All data was analyzed using a nonlinear least-squares fitting program with a Gaussian–Lorentzian product function and an asymmetric tail on the primary peak to account for conduction band interaction.<sup>11</sup> A mixing ratio of 0.7 was used for all peaks. Atomic ratios reported in Table 2 were calculated from the XPS survey spectra after correcting the relative peak areas by sensitivity factors based on the transmission characteristics of the Physical Electronics SCA.<sup>12</sup> The area of sample probed by the spectrometer was 1 mm<sup>2</sup>. The data

(9) Dubinin, M. M.; Stoeckli, H. F. *J. Colloid Interface Sci.* **1980**, *75* (1), 34.

(10) Kozłowski, C.; Sherwood, P. M. A. *J. Chem. Soc., Faraday Trans. 1* **1984**, *80*, 2099.

(11) Sherwood, P. M. A. *Practical Surface Analysis by Auger and Photoelectron Spectroscopy*; Briggs, D., Seah, M. P., Eds.; Wiley: London, 1983; Appendix 3.

(12) Chastain, J.; King, Jr., R. C. *Handbook of Photoelectron Spectroscopy*; Perkin-Elmer, Physical Electronics Division: Eden Prairie, MN, 1995.

(8) McEnaney, B. *Carbon* **1987**, *25*, 49.

**Table 2. Number and Type of Functional Groups for the Treated and Untreated ACFs as Calculated Using XPS**

| sample | phenolic hydroxyls (mmol/g) | quinones (mmol/g) | carboxylic acids (mmol/g) | % O XPS | ratio <sup>a</sup> |
|--------|-----------------------------|-------------------|---------------------------|---------|--------------------|
| ACF-10 | 2.57                        | 0.78              | 1.57                      | 7.87    | 0.84               |
| ACF-15 | 1.35                        | 0.4               | 1.90                      | 5.84    | 0.74               |
| ACF-25 | 0.98                        | 0.26              | 1.34                      | 4.13    | 0.97               |
| 10-A1  | 5.59                        | 2.34              | 4.24                      | 19.46   | 1.11               |
| 10-A2  | 10.32                       | 0.52              | 4.55                      | 24.62   | 1.08               |
| 15-A1  | 9.64                        | 0.4               | 4.20                      | 22.78   | 0.98               |
| 15-A2  | 7.15                        | 0.66              | 7.69                      | 24.8    | 1.13               |
| 25-A1  | 5.32                        | 1.35              | 7.68                      | 22.96   | 1.11               |
| 25-A2  | 4.29                        | 0.55              | 11.60                     | 26.31   | 1.07               |
| 15-C1  | 3.30                        | 2.70              | 1.98                      | 12.77   | 1.02               |
| 15-C2  | 3.25                        | 2.32              | 10.12                     | 25.1    | 1.15               |
| 15-D1  | 3.12                        | 0.82              | 2.27                      | 9.95    | 0.97               |
| 15-E1  | 5.62                        | 0.46              | 1.22                      | 11.68   | 0.67               |

<sup>a</sup> The total oxygen content is compared for values measured using XPS to those determined from elemental analysis.

shown in Table 2 is reported assuming the region probed by XPS was homogeneous.

#### Diffuse Reflectance Infrared Spectroscopy (DRIFTS).

A Magna IR TM Spectrometer 550 (Nicolet) was used in reflectance mode to measure the infrared spectrum of the ACFs and to identify their chemical functionality. Data acquisition was performed automatically using standard software (Omnice). The ACFs were dried at 150 °C under vacuum prior to IR evaluation. The sample was ground with a mortar and pestle (2 min) and mixed with ground KBr powder. A baseline was measured using ground KBr powder; this was subsequently subtracted from the measured sample spectrum. The sample chamber in the spectrometer was purged with nitrogen (20 min) from which carbon dioxide and water were removed. For a typical run, 1000 scans were obtained at a resolution of 2 cm<sup>-1</sup> using triangular apodization.

**Ammonia and Acetone Adsorption Isotherms.** The adsorption of acetone and ammonia was measured thermogravimetrically using a TGA 951 (TA Instruments, New Castle, DE) interfaced with a TA Instruments 2100 System Computer. Mass flow controllers (Tylan General) were used to dilute standards (1000 parts per million by volume (ppmv) acetone in ultrahigh purity N<sub>2</sub> and 5000 ppmv ammonia in UHP N<sub>2</sub>) to lower concentrations. Experiments were also conducted at higher temperatures to determine temperature effects on desorption. The temperature was ramped to the desired level (maximum of 125 °C) and held until equilibrium values were obtained. For these temperature studies the concentration of ammonia was 5000 ppmv while the concentration of acetone was 1000 ppmv.

## Results and Discussion

**Oxidation of Carbons.** A number of carbonaceous materials have been oxidized including carbon fibers,<sup>13,14</sup> carbon blacks,<sup>15</sup> and activated carbons<sup>16</sup> using a variety of aqueous and nonaqueous treatments. Typically, the degree of oxidation increased with increasing reaction treatment as the oxidant etched the carbon structure resulting in the evolution of carbon monoxide and carbon dioxide. Our experiments also indicate that the degree of oxidation was dependent on the time and strength of treatment as shown in Table 1. For instance, treatment of the ACFs in concentrated nitric/sulfuric

acid, boiling nitric acid, or air at 600 °C created the most oxygen-containing functional groups while treatments with less aggressive sulfuric acid, hydrogen peroxide, or acetic acid created fewer. In all cases, treatment of the ACFs in aqueous medium resulted in a weight increase from added oxygen ranging from 0.70% to 17% with H<sub>2</sub>SO<sub>4</sub>/HNO<sub>3</sub> having the greatest increase. In contrast, treatment of the ACFs in air resulted in a decrease in the sample weight from 6% to 53% for reaction temperatures of 400 and 600 °C, respectively. Thus, reaction of the ACFs in aqueous solution is less aggressive. One notes an increase in weight due to oxygen chemisorption while oxidation of the ACFs in air is accompanied by weight loss due to the rapid gasification of the structure through loss of CO and CO<sub>2</sub>.<sup>1</sup>

**Effect of Oxidation on the Pore Structure of ACFs.** Very little previous work has been reported to demonstrate how oxidation affects the porous structure of ACFs. Our work shows a correlation between the extent of oxidation, pore volume, and surface area. Nitrogen BET surface area data is shown for the treated and untreated ACFs in Table 1. Aqueous phase oxidation lowered ACF surface area while air oxidation caused an increase in surface area. In addition, micropore size and volume of the treated and untreated ACFs was calculated from the experimental nitrogen adsorption isotherms at 77 K using the Dubinin–Radushkevich (DR) equation (Table 1). We observe that the aqueous oxidized ACFs average micropore size changed very little from the original value while the pore volume decreases with increasing oxidation. One also notes that the pore volume and surface area are linearly proportional to one another such that the surface area decreases with decreasing pore volume. These results are in good agreement with those reported by Barton and co-workers for granular active carbon.<sup>3</sup> The average micropore size was independent of oxygen content, thus it appears that the oxygen containing functional groups are not “constricting” the pores. One could argue that the surface area and pore volume decrease with aqueous oxidation due to the added weight of oxygen-containing groups. Since these values are reported as normalized to grams of ACF, an increase in weight from the oxidation process will result in lower surface area/pore volume values per unit weight. Treatment of the ACFs in air increases both the average micropore size and micropore volume due to the rapid etching of the carbonaceous skeleton. This results in the concurrent increase in surface area.

**Effect of Oxidation on Surface Chemistry.** It is generally accepted that oxidation of carbons produces oxygen-containing functional groups at the edge sites of the graphitic planes. The type and number of oxygen containing functional groups have been the subject of much interest and debate in this field.<sup>17</sup> DRIFTS was used to qualitatively identify the chemical functionality of untreated and oxidized fibers. All samples in this study were evaluated by DRIFTS and representative spectra are shown in Figure 1. Figure 1 shows the differences in infrared absorption of as-received fibers (ACF-15), fibers oxidized with concentrated nitric/sulfuric acids (15-A2), and fibers reacted with acetic acid

(13) Barton, S. S.; Koresh, J. E. *J. Chem. Soc., Faraday Trans. 1* **1983**, *1*, 79 (5), 1173.

(14) Brewis, D. M.; Comyn, J.; Fowler, J. R.; Briggs, D.; Gibson, V. *Fiber Sci. Technol.* **1979**, *12* (1), 41.

(15) Given, P. H.; Hill, L. W. *Carbon* **1969**, *7* (6), 649.

(16) Barton, S. S.; Dacey, J. R.; Evans, M. J. B. *Colloid Polym. Sci.* **1982**, *260* (7), 726.

(17) Proctor, A.; Sherwood, P. M. A. *Carbon* **1983**, *21* (1), 53.

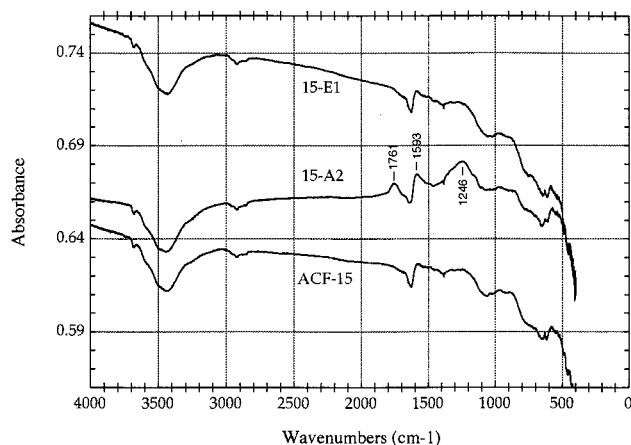
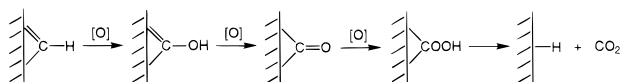


**Figure 1.** DRIFTS spectrum for ACF-15, 15-A2, and 15-E1.

(15-E1). As expected, acetic acid had little effect on the fiber due to its poor oxidizing ability. However, several new peaks appeared in the spectrum of the  $\text{HNO}_3/\text{H}_2\text{SO}_4$  treated fibers and were appropriately labeled. Notable characteristic peaks for this material are at  $1761\text{ cm}^{-1}$  (carbonyl stretching of quinones and carboxylic acids),  $1593\text{ cm}^{-1}$  (C=C stretching in the form of aromatic rings), and  $1246\text{ cm}^{-1}$  (C–O stretches presumably from both carboxylic acid groups and phenolic hydroxyls). Other peaks include  $972$ ,  $856$ , and  $579\text{ cm}^{-1}$  that account for –CH bending. While it was not possible to obtain quantitative information from the DRIFTS scans performed, it was possible to identify the oxygen-containing functionality as primarily consisting of carboxylic acids, quinones, and phenolic hydroxyls. This result agrees well with the generally accepted method shown below for stepwise oxidation of carbons:<sup>18–20</sup>



Experiments performed by Puri also determined that these three groups typically dominate an oxidized pore surface.<sup>1</sup>

In addition, XPS was used to confirm the types of oxygen-containing functional groups and to measure their relative abundance at the fiber surface for both oxidized and untreated fibers. For convenience the C1s was used for this determination although the O1s peak could also be used. Figure 2 is the C1s region of 15-A2 and is representative of the more than 100 spectra we have collected on the treated and untreated fibers. Three characteristic oxide peaks were observed in these spectra which are indicative of phenolic hydroxyls, quinones, and carboxylic acids. For consistency, the oxide peaks of all spectra were fitted by shifting them 1.55, 3, and 4 eV from the main amorphous carbon peak, respectively. In addition, a shake-up peak due to the  $\pi$ -bonding of unsaturated sites can be found shifted 6 eV from the main peak. These assignments are in agreement with previous authors who have studied oxidized carbon

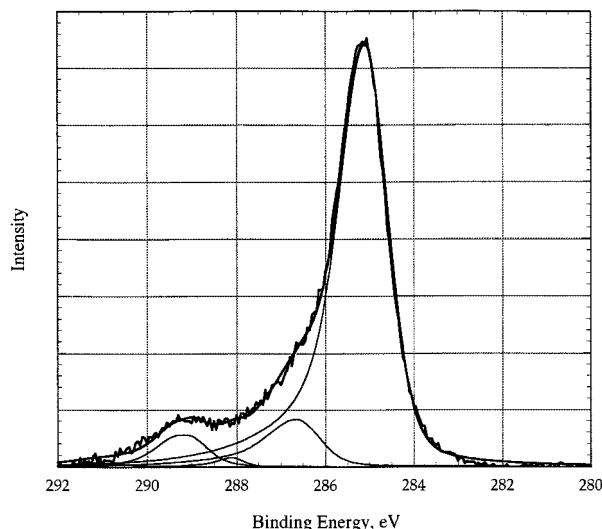


**Figure 2.** XPS C1s region for 15-A2.

surfaces with XPS.<sup>12,17,21</sup> The relative amount of each of these groups was determined by integrating the area under the peak after a proper subtraction of the baseline. Table 2 provides a summary of the relative number and type of oxygen-containing groups.

The amount of all these groups increased with oxidation treatment while no treatment created only specific types of functional groups. The number of quinones and phenolic hydroxyls followed no trend with increasing reaction temperature or time while the number of carboxylic acid groups continued to rise with increasing reaction temperature or time.

In contradiction to the work of Dimotakis et al.,<sup>22</sup> we have shown through extensive testing that the amount of oxygen measured using XPS agrees, within experimental error, with the amount of oxygen determined using elemental analysis (Table 2). This suggests that the oxidation treatment is uniform throughout the fiber and is not substantially different at the surface as compared to the bulk.

**Effect of ACFs Oxidation on Adsorption.** Earlier work has shown that oxidized activated carbons exhibit enhanced adsorption of various contaminants including phenol, aniline, and alizarin yellow from ethanol solutions over their nonoxidized ACF counterparts.<sup>23</sup> However, this enhanced adsorption is suppressed in aqueous solution due to the hydrophilic nature of the oxidized carbon surface. Thus, oxidation of activated carbons was shown to be detrimental for the adsorption of contaminants from water. Our group studied adsorption of saturated gases onto oxidized and nonoxidized ACFs, but the lower pore volumes that resulted from oxidation resulted in poor performance.<sup>5</sup> In this paper we have extended this work to demonstrate that oxidized ACFs provide for enhanced adsorption of polar contaminants such as acetone and for basic contaminants such as ammonia while utilizing much lower (and more realistic) concentrations. We have also laid the foundation for

(21) Polovina, M.; Babic, B.; Kaluderovic, B.; Dekanski, A. *Carbon* **1997**, *35* (8), 1047.

(22) Dimotakis, E. D.; Cal, M. P.; Economy, J.; Rood, M. J.; Larson, S. M. *Environ. Sci. Technol.* **1995**, *29* (9), 1876.

(23) Ogata, Y.; Matsumura, Y.; Takahashi, H. *Colloid Polym. Sci.* **1979**, *257*, 1232.

(18) Horie, K.; Murai, H.; Mita, I. *Fiber Sci. Technol.* **1976**, *9*, 253.

(19) Weinberg, N. L.; Reddy, T. B. *J. Appl. Electrochem.* **1973**, *3*, 73.

(20) Rivin, D. *Rubber Chem. Technol.* **1963**, *36*, 729.

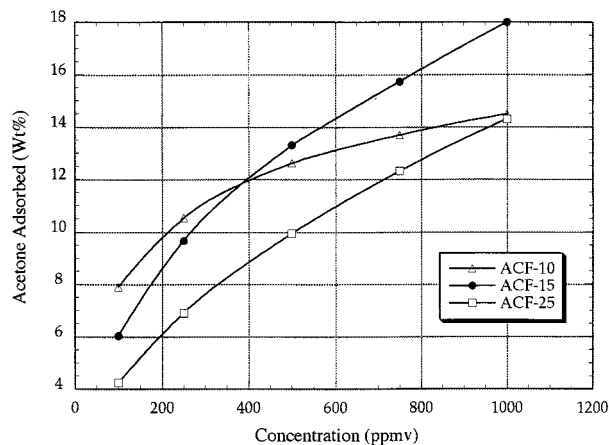


**Figure 3.** Acetone adsorption isotherms at 25 °C for ACFs.

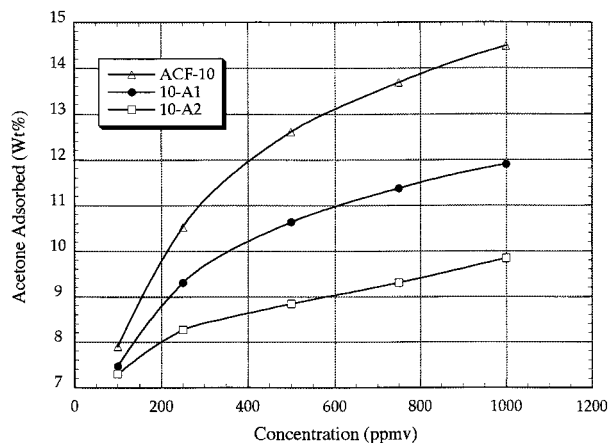


**Figure 4.** Acetone adsorption isotherms at 25 °C for ACF-10, 10-A1, and 10-A2.

pore property optimization for removal of such contaminants.

**Adsorption of Acetone.** It is not surprising that in highly oxidized fibers, many polar groups are present primarily in the form of carboxylic acids. We believe these groups to be the most beneficial for adsorption of acetone due to dipole interactions.

The acetone adsorption isotherms are shown for the untreated ACFs in Figure 3. A crossover phenomenon is observed and can be explained by the relationship between pore size and pore volume of the ACFs. The lower surface area (smaller pore size) ACF-10 adsorbs better at low concentration due to a higher overlap in potential between opposite pore walls which binds the molecule more tightly. With the wider pores of the ACF-15 and ACF-25, the potential overlap of the pore walls is less and leads to lower amounts of adsorption at low concentration. At higher concentrations, the ACF-10 isotherm begins to level, indicating that there is little available pore volume remaining for adsorption. The ACF-15 and ACF-25 isotherms are still rising as the concentration increases due to the availability of additional pore volume.

When the ACF-10 is oxidized, its adsorption capacity for acetone decreases due to a decrease in the total micropore volume (Figure 4). The small pore size of the ACF-10 provides enough driving force to fill most of its pore volume even with no treatment. In this case, oxidation cannot increase acetone adsorption because

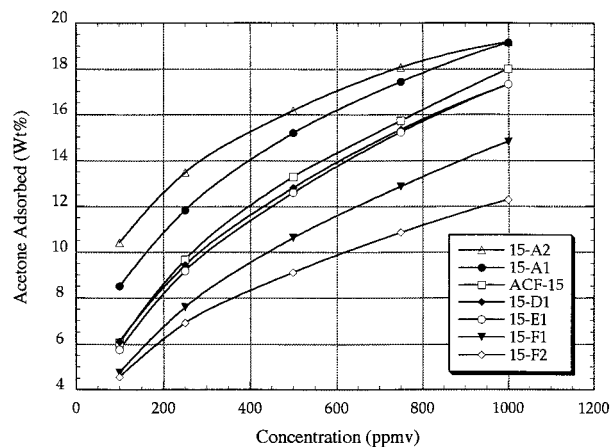


**Figure 5.** Acetone adsorption isotherms at 25 °C for ACF-15 series.

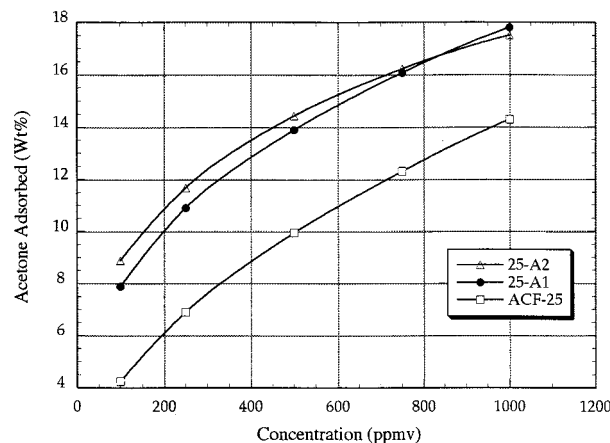


**Figure 6.** Acetone adsorption isotherms at 25 °C for ACF-25, 25-A1, and 25-A2.

total available pore volume is the limiting feature. Tamon et al. observed similar behavior with oxidized granular carbon of comparable surface area.<sup>6</sup> As the extent of oxidation increased, the total pore volume decreased, leading to decreased acetone capacities. In contrast, treatment of the higher surface area ACFs in concentrated  $\text{HNO}_3/\text{H}_2\text{SO}_4$  generally increases the amount of acetone adsorbed as seen in Figures 5 and 6.

Figure 5 shows the acetone adsorption isotherms for various oxidation treatments. Treatment of the ACF-15 in  $\text{H}_2\text{O}_2$  or  $\text{CH}_3\text{COOH}$  decreased the overall effectiveness of the samples for adsorption of acetone. The amount of acetone adsorbed by these samples was slightly higher than the ACF-15 at 100 ppmv and was inferior to the ACF-15 at higher concentrations. Again, reduced pore volume is a contributing factor but XPS indicates lower amounts of carboxylic acid groups formed from these treatments (thus adsorption of acetone is impaired). The total available pore volume of the oxidized ACFs is lower than untreated ACFs and at higher concentrations, the oxidized pores simply become saturated with adsorbate. Surprisingly, treatment of the ACF-15 in air also decreased the adsorption capacity of the oxidized samples for acetone. Although the sample produced at 600 °C had high oxygen content, it is reasonable to assume that the acetone adsorption capacities are greatly offset due to an increase in pore size.

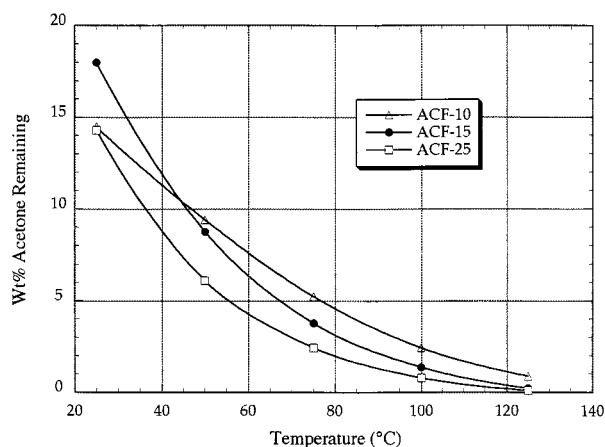


**Figure 7.** Acetone adsorption at temperatures from 25 °C to 125 °C for ACF-10, ACF-15, and ACF-25 at an acetone concentration of 1000 ppmv in nitrogen.

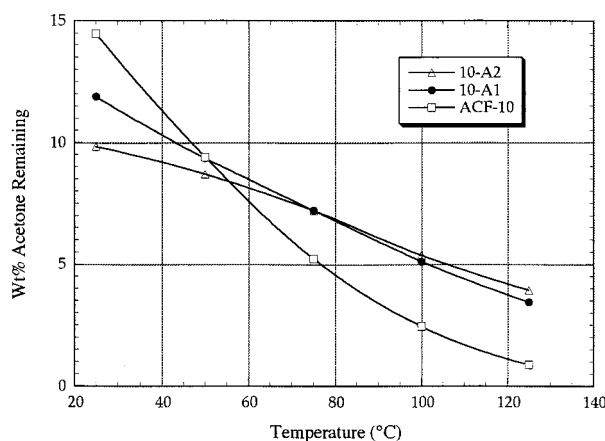


**Figure 8.** Acetone adsorption at temperatures from 25 °C to 125 °C for ACF-10, 10-A1, and 10-A2 at an acetone concentration of 1000 ppmv in nitrogen.

Sulfuric/nitric acid oxidations had only a modest effect on the adsorption properties of the ACFs for acetone at ambient conditions (Figure 5). Nitric acid treatments provided very similar results and are therefore not depicted in Figure 5. The enhanced adsorption is presumably caused by the dipole-dipole interactions from the carboxylic acid groups and the polar acetone molecule. Although the adsorption capacity of the oxidized fibers for acetone is increased over their as-received precursor fibers, in many cases it is possible to obtain this level of increased adsorption solely through modification of the pore size and pore volume (Figure 3).

The desorption properties of the ACFs and oxidized ACFs were studied for acetone by utilizing equilibrium values at temperatures up to 125 °C. At temperatures above 40 °C, the amount of acetone retained is higher for smaller pore sized fibers, as shown in Figure 7. The smaller pores are more effective at binding the adsorbate between the pore walls as the temperature increases. The adsorbed amount decreases with increasing temperature as the binding energies of the adsorbate are overcome with increasing thermal motion.

As shown in Figures 8 and 9, the oxidized ACFs have improved acetone retainment as the temperature is increased. The number of oxygen functional groups is generally a more critical factor than pore size for

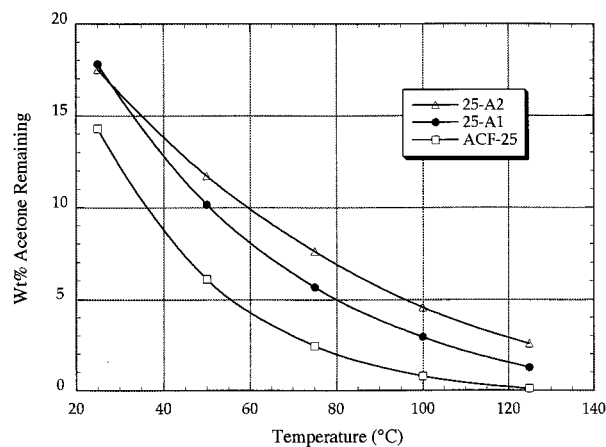


**Figure 9.** Acetone adsorption at temperatures from 25 °C to 125 °C for ACF-25, 25-A1, and 25-A2 at an acetone concentration of 1000 ppmv in nitrogen.

adsorption at higher temperatures since physical adsorption is no longer strong enough to maintain high capacity. Therefore, chemical interaction of polar groups on the oxidized sample with the polar acetone contaminant becomes necessary. This same type of trend would also occur at much lower concentrations as physical adsorption becomes small compared to pore chemistry effects.

In summary, both a smaller pore size and an increase in the oxygen containing groups (carboxylic acids) increase the adsorption energy of ACFs for polar contaminants. This energy of adsorption, however, will only result in improved capacity provided that enough pore volume is available. As seen from Figures 4–6, the highest levels of acetone adsorption are observed for the oxidized ACF-15 by balancing the pore volume and the number of oxygen functional groups with a modest pore size. To maintain adsorption at higher temperatures, the pore volume is less of a contributing factor since lower amounts of contaminant are retained. Thus, both a smaller pore size and an increased number of oxygen containing functional groups are needed to enhance capacity.

**Adsorption of Ammonia.** It was predicted that oxidized ACFs, due to the acidic nature of the carboxylic acid groups and phenolic hydroxyls, would also exhibit enhanced adsorption for basic contaminants. Therefore, the adsorption of ammonia onto as-received and oxidized ACFs was also examined. Not surprisingly, all precursor ACFs have very low adsorption capacity for ammonia since it is a relatively low boiling point gas. Figures 10–12 demonstrate how a concentrated nitric/sulfuric acid treatment greatly enhances the ammonia adsorption capacity of ACFs. For any given ACF, the amount of ammonia adsorbed increased with increasing acid treatment time. Figure 11 shows ammonia adsorption isotherms for various oxidation treatments. This figure demonstrates that the amount of ammonia adsorbed increased with increasing reaction time/strength. ACF-15 fiber treated in concentrated nitric/sulfuric acid for 1 h exhibited a 30-fold improvement (the best system) in adsorption of ammonia compared to the untreated ACF-15. ACF-15 treated in acetic acid or H<sub>2</sub>O<sub>2</sub> showed a modest increase in adsorption capacity for ammonia from 2.3 to 3.0 times, respectively, over the untreated ACF-15. Finally, treatment of the ACF15 with air

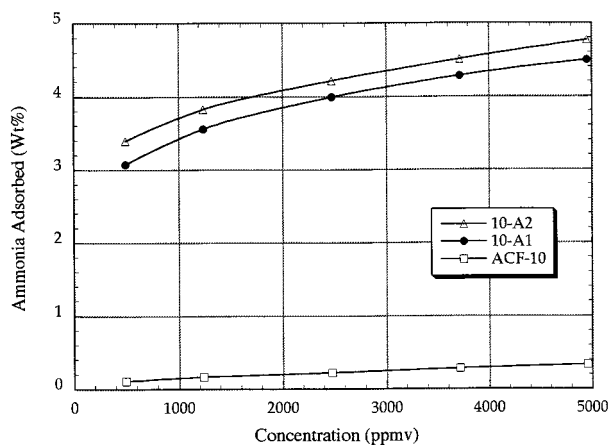


**Figure 10.** Ammonia adsorption isotherms at 25 °C for ACF-10, 10-A1, and 10-A2.

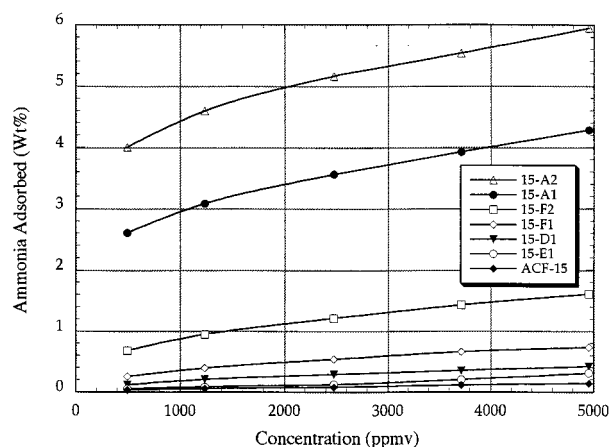


**Figure 11.** Ammonia adsorption isotherms at 25 °C for ACF-15 series.

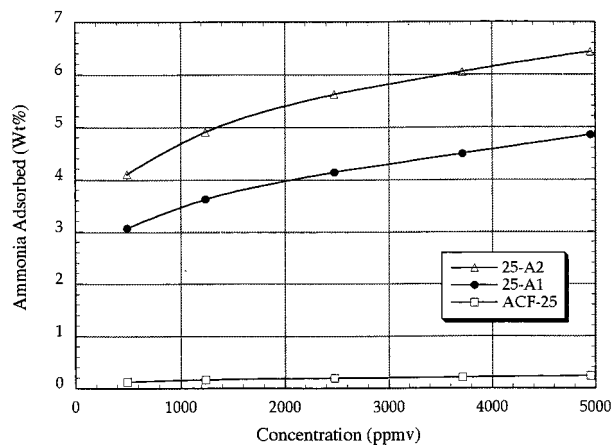


**Figure 12.** Ammonia adsorption isotherms at 25 °C for ACF-25, 25-A1, and 25-A2.

increased its adsorption capacity from 5.4 to 8.6 times compared to no treatment. Tamon et al. also observed enhanced ammonia adsorption with oxidation of granular carbon.<sup>6</sup> However, the activated carbon fibers in this study have higher amounts of surface functionality in comparison to Tamon's reported values due to higher achievable surface areas. This gives the fibers a moderate advantage for increased adsorption capacity of ammonia.

Again, the desorption properties of ammonia were studied using the treated and untreated ACFs at

**Table 3. Energy of Adsorption and Desorption of Acetone, As Calculated with Temperature, for a Series of ACFs**

| sample | energy of adsorption (kJ/mol) | energy of desorption (kJ/mol) |
|--------|-------------------------------|-------------------------------|
| ACF10  | 19.4                          | 9.05                          |
| ACF15  | 14.5                          | 7.29                          |
| ACF25  | 13.7                          | 6.83                          |
| 15-A1  | 17.7                          | 9.43                          |
| 15-A2  | 19.3                          | 12.2                          |

temperatures from 25 to 125 °C. At higher temperatures, the retention trends are the same as those previously reported for acetone (figures not shown for brevity). Granular carbon exhibited irreversible ammonia adsorption in contrast to the ACFs completely reversible adsorption. A possible explanation for this behavior lies in the precursor material used to prepare the activated carbon. Granular carbon often contains metal impurities that may react and chemisorb the ammonia contaminant while ACFs are prepared from relatively pure phenolic precursors containing little impurity.

To summarize, the oxidized carbon fiber provided as much as 30 times the adsorption capacity as that of the best untreated ACF. Samples with very high oxygen contents tended to have higher adsorption capacities for ammonia on the basis of the direct interaction of the carboxylic acid and phenolic hydroxyl functional groups with the basic contaminant. Since ammonia is a relatively low boiling point gas, the pore size and pore volume has very little effect on its adsorption. Previous work explains this phenomena in more detail.<sup>24</sup> Even the smallest pore size materials (highest potential overlap) exhibit very poor adsorption of ammonia. Therefore, one of the few means to increase the adsorption capacity for low boiling point adsorbates such as ammonia is to tailor the surface chemistry.

**Analysis of Adsorption Energies.** This work demonstrates that surface chemistry becomes important to maintain adsorption of contaminants at higher temperatures. The amount of adsorption of polar and basic contaminants increases with increasing oxygen content of the fibers oxidized under aqueous conditions. This increased adsorption occurs for both polar and acidic contaminants regardless of the boiling point or concentration of the adsorbate.

Previously, we demonstrated how eq 1 is used to determine the energy of adsorption utilizing various concentrations for different adsorbates. This equation can be rearranged to analyze the desorption of contaminants as a function of temperature. For this calculation, the term  $\log^2(P_0/P)$  becomes a constant and the desorption energy is calculated from the slope of the best fitting line on a plot of  $\log(W)$  vs  $T^2$ . The adsorption and desorption energies that resulted for one set of samples are listed in Table 3 and are used to gauge the effectiveness of tailored pores on adsorption.

From Table 3, one notes that the adsorption energy increases with decreasing pore size for the ACFs as calculated as a function of temperature or concentration. This agrees with the concept of small pores having a

(24) Mangun, C. L.; Daley M. A.; Braatz R. D.; Economy J. *Carbon* **1998**, *36* (1–2), 123.

greater overlap in potential. One also observes that the adsorption energies of the oxidized ACFs are higher than those of the untreated ACFs, indicating that pore surface chemistry provides for enhanced interaction regardless of temperature or concentration.

**Thermal Stability.** Thermal stability of oxygen containing functional groups is a very important parameter. In industrial use, samples would need to be regenerated multiple times so it is important that the oxygen groups are stable at regeneration temperatures. Although no data was presented, fibers that exhibited enhanced adsorption could be regenerated at low temperatures of 200 °C where all adsorbed contaminants were completely desorbed. Experiments with TGA indicated little weight loss at these temperatures. Puri found that surface oxygen complexes on carbons are generally stable, even under high vacuum, to about 250 °C.<sup>1</sup>

### Concluding Remarks

Oxidation of carbon fibers can markedly improve the adsorption of many environmental contaminants. The effects of oxidation on pore structure and chemistry have been identified and can be used to tailor ACFs for removal of specific contaminants. This knowledge is particularly important in terms of adsorbent regeneration, and the materials described here can be fully regenerated below their decomposition temperatures.

**Acknowledgment.** We thank NSF (Grant # DMR-9208545) for supporting this research work. XPS analysis was carried out at the Center for Microanalysis of Materials at the University of Illinois at Urbana-Champaign, which is supported by the United States Department of Energy under grant DEFG02-ER-45439. CM990123M